Supplement of Solid Earth, 16, 1205–1226, 2025 https://doi.org/10.5194/se-16-1205-2025-supplement © Author(s) 2025. CC BY 4.0 License.





## Supplement of

# Dissolution-precipitation creep in polymineralic granitoid shear zones in experiments – Part 2: Rheological parameters

Natalia Nevskaya et al.

Correspondence to: Natalia Nevskaya (natalia.nevskaya@yale.edu)

The copyright of individual parts of the supplement might differ from the article licence.

### S1 Grain size analysis from Mastersizer for fine-grained gouge material

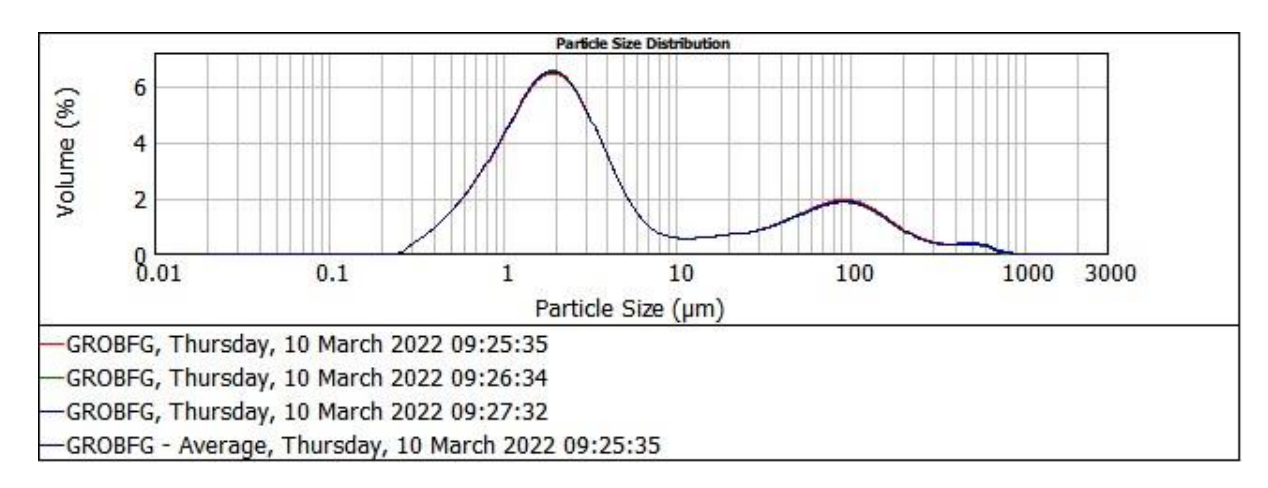
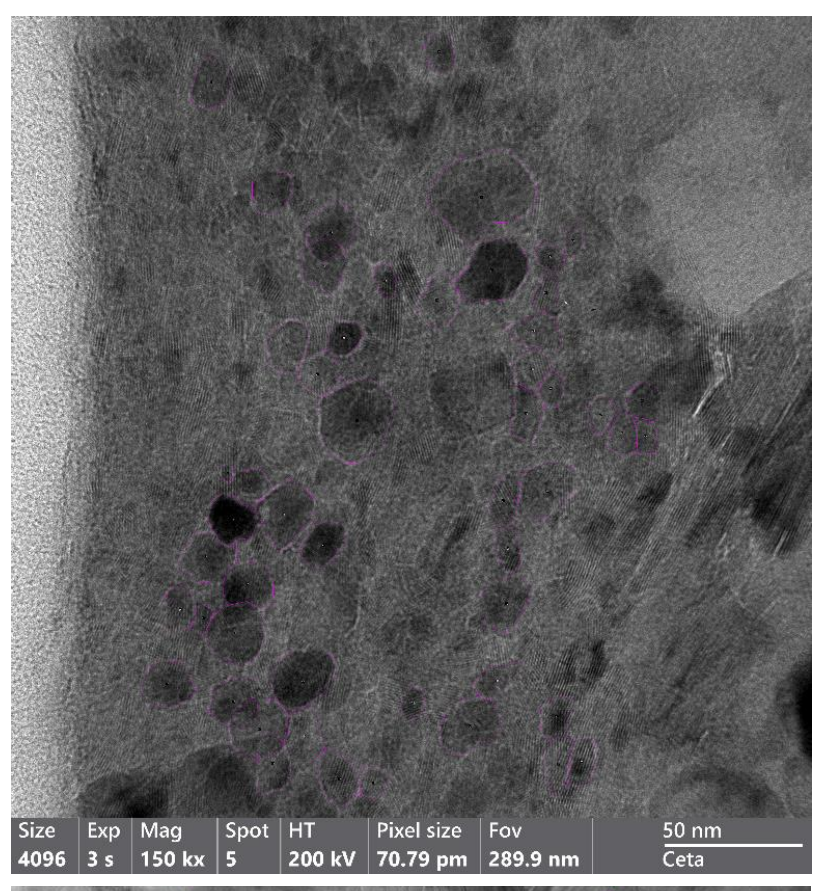
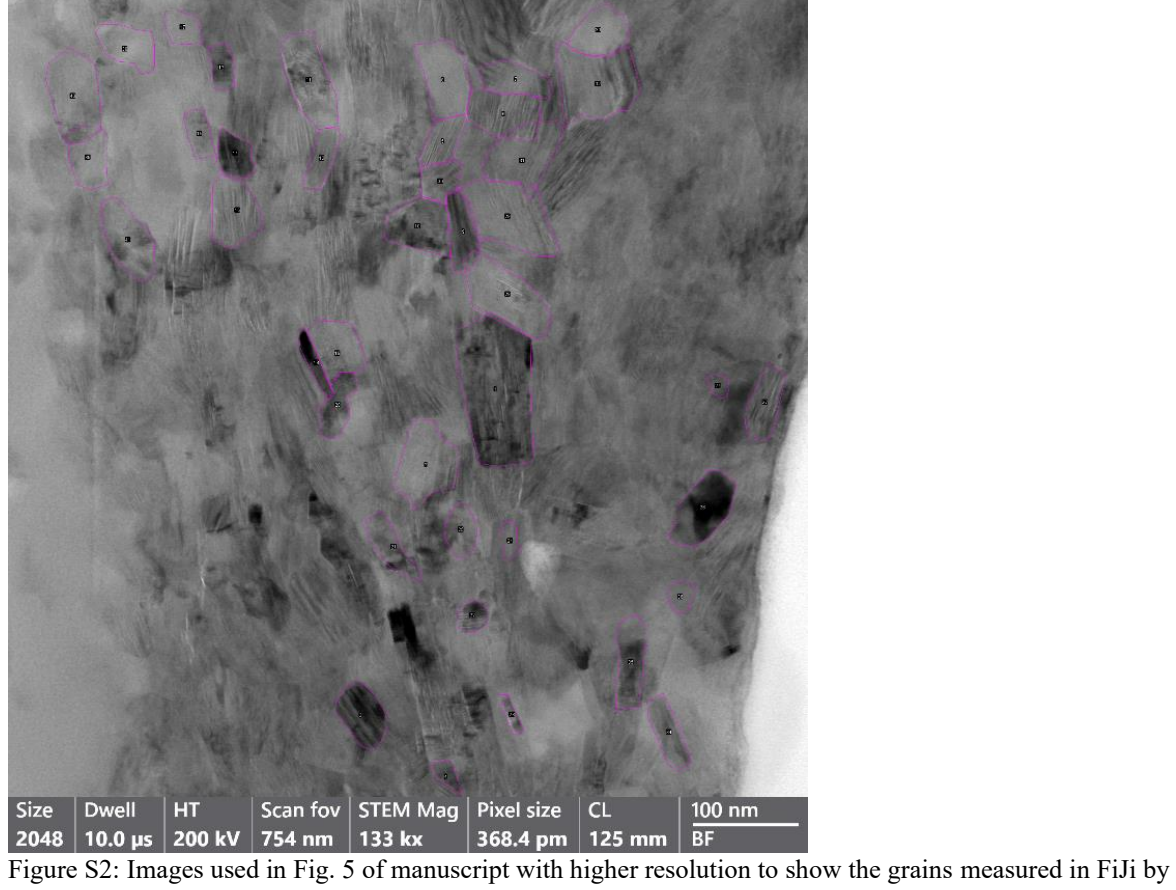


Figure S1: Plot of grain size distribution as measured by Mastersizer in vol%. All material was sieved such that grain sizes of  $>20~\mu m$  must be due to clustering in suspension.

## S2 Example TEM images for grain size analysis with FIJI





ImageJ.

#### S3 Details for calculations of mechanical data

In the following sections, detailed information is given for considerations and parameters of the calculations of mechanical data and flow law parameters.

#### S3.1 HK-correction impact on flow law parameter calculations

As the mechanical data of the apparatus can be corrected by different methods we would like to present a comparison of the stress values obtained with different corrections and how these corrections affect consequent calculations of n-values. In the following Table S1, we show the strain rates and stresses we have calculated. The maximum range for the stress exponent n using different corrections covers approximately n=1.4 to 1.8. This is an important result, because it demonstrates that the interpretations of our study are robust and not dependent on individual correction procedures. In our interpretations we only deal with the range of values not individual numbers.

In particular, we would like to discuss possible concerns regarding the Holyoke and Kronenberg (2010) (H&K2010) molten (MSC) (Equation S1) and solid salt cell (SSC) (Equation S2) assembly corrections:

$$\sigma_{gas} = 0.73 \times \sigma_{GriggsMSC}$$
 (+/-30 MPa)

$$\sigma_{gas} = 0.73 \times \sigma_{GriggsSSC} - 48 \text{ MPa}$$
 (+/-30 MPa)

We have performed all experiments in a solid salt cell and have applied the correction of the molten salt cell. This appears as an application of the wrong correction. However, the slopes of the two corrections are identical, and the only difference is the shift of values along the y-axis. If the solid salt correction is applied to our samples, it will result in negative differential stress values for the slowest strain rate steps (i.e. low sample strengths). This situation has arisen in our lab and in other labs before (oral communication Greg Hirth), and this is the main reason, why the correction procedure by Holyoke and Kronenberg (2010) often is not applied.

As Holyoke and Kronenberg discuss in their (2010) paper, some potential problems of the calibration lie in the mating of pistons in the Griggs apparatus, which is not designed to be operated at the low confining pressures that were required for their calibration experiments to be correlated with a gas apparatus. For the reason to avoid negative stresses for  $\sigma_1$  -  $\sigma_3$  (such values would imply an extension experiment, but we have performed only shortening experiments), we have tried to apply the H&K (2010) correction of the slope of the calibration curve without the shift along the y-curve. This correction is the molten salt calibration (again: the slope is identical to that of the solid salt correction). Our highest n-value results from calculating the stress exponent without taking the slowest strain rate step, as it appears negative after applying the H&K2010-SSC correction. This questions the validity of the lowest stress. However, as we measured this value in a strain rate stepping experiment (the advantage of such experiments is that all stress values are measured with respect to the same reference value of the hit point, i.e. avoiding different friction terms in different experiments), we believe that the data point should be used as an indicator for the stress sensitivity. Hence, we used the correction for a MSC, as the SSC correction does not affect the slope and only a vertical offset with respect to the MSC. Also, as in Table S1, the influence of this correction on n, due to the very low stresses we measured, lies beyond the decimals shown/relevant.

Furthermore, the experiment at the higher temperature of 725°C gives us the smallest stress exponent of n=1.4. It could mean that the deformation mechanisms at higher temperature change. However, as shown by microstructures (see companion paper 1, Nevskaya et al. 2025a), the deformation mechanism based on microstructural criteria remains the same. This observation is the basis for our reasoning for averaging the calculated stress exponents between the 650°C and 725°C experiments (Table S1). The averaging is performed by weighting the n-values by the number of datapoints through which the regression line was fitted. Overall, this procedure was made to take more data into account. But, as mentioned above, even considering a range of n values of 1.4 to 1.8 is not significant for our interpretations and discussion in the manuscript.

Then the resulting n-values are averaged, weighted by the amount of datapoints in each set. Note that experiment 615NW and 618NW are Type I experiments with a pre-fracture and the other experiments are fine-grained gouge simple shear experiments. Experiment 615NW showed slightly different microstructures and was not displayed in the first version of the manuscript, hence the n-value differs slightly. However, here we still show it to estimate the largest range of steady state stresses at the end of the experiment, which also correspond to the final microstructures. A regression is performed on two datasets - 650 and 725°C. Table S1: Measured and corrected stress measurement of different experiments and the resulting calculated stress exponents n. The stresses given here are uncertainty within our study.

Exp. No	Exp. No Temp. (°C)	Strain rate (s-1)	equivalent strain rate (s-1)	Shear stress (MPa)	Shear Stress friction corrected (MPa)	Equiv./Dif f stress (MPa)	Diff stress- Friction corrected (MPa)	Shearstr. Friction HK, SSC (MPa)	Diffstress friction HK, SSC (MPa)	Shearstr. Friction HK, MSC (MPa)	Diffstress friction HK, MSC (MPa)	Weights
673NN	650	4.52E-05	5.22E-05	46.26	30.42	92.52	60.84	-1.79	-3.58	22.21	44.42	
673NN	650	2.91E-04	3.36E-04	195.83	186.55	391.65	373.10	112.18	224.37	136.18	272.37	
673NN	650	3.07E-03	3.55E-03	447.76	411.49	895.51	822.98	276.39	552.77	300.39	600.77	
673NN	650	3.96E-04	4.58E-04	192.38	142.38	384.75	284.76	79.94	159.88	103.94	207.88	
618NW*	, 650	1.07E-03	1.23E-03	334.46	274.14	671.20	544.78	175.97	349.69	200.12	397.69	
615NW*	, 650	9.65E-04	1.11E-03	232.17	225.69	516.90	398.55	137.57	242.94	164.76	290.94	
	calci	calculated n-value	a)	1.78	1.54	1.78	1.54	1.82	1.75	1.54	1.54	9
677NN	725	4.85E-05	5.59E-05	18.94	11.45	37.88	22.89	-15.65	-31.29	8.35	16.71	
<b>677NN</b>	725	4.66E-04	5.38E-04	100.24	91.11	200.48	182.21	42.51	85.01	66.51	133.01	
677NN	725	4.78E-03	5.52E-03	275.21	253.19	550.42	506.38	160.83	321.66	184.83	369.66	
677NN	725	4.89E-04	5.65E-04	131.05	93.74	262.10	187.48	44.43	88.86	68.43	136.86	
	calci	calculated n-value	Ð	1.60	1.40	1.60	1.40	1.76	1.76	1.40	1.40	4
	Š	weighted avg		1.71	1.48	1.712	1.48	1.80	1.76	1.48	1.48	

#### S3.2 Baseline force – correction of load by piston friction calculations:

Another uncertainty that needs to be addressed is the calculation of the hit point at different strain rates. It is inferred that the force during the run-in stage of the experiment before the hit point stays constant at a given displacement rate (often termed "friction") but could change depending on the vertical displacement rate (Proctor et al. 2016), see also Tarantola et al. (2010). This topic still is a source of debate in the scientific community applying solid-confining-medium-apparatus, as has been shown in a workshop at Orleans in 2020, where most of such apparatus users were present. For most typical displacement rates, the effect on the measured force has been found negligible by M. Pec 2014 in their tests in the same apparatus that we used in this study. Only at very slow rates (Tarantola et al. 2010) the viscous components on the run-in slope are reduced. Also, Proctor, 2016 have found that the change of force for different vertical velocities at slow rates is very low, being only 3-5MPa for one order of magnitude change. Based on these assumptions, we did not perform additional run-in steps, also because it was very important for this study to have pristine microstructures. However, from the experimental series that we performed, we could investigate the run-in curves of different experiments at different strain rates. In Figure S3 we show the plots for displacement – force curves of complete experiments.

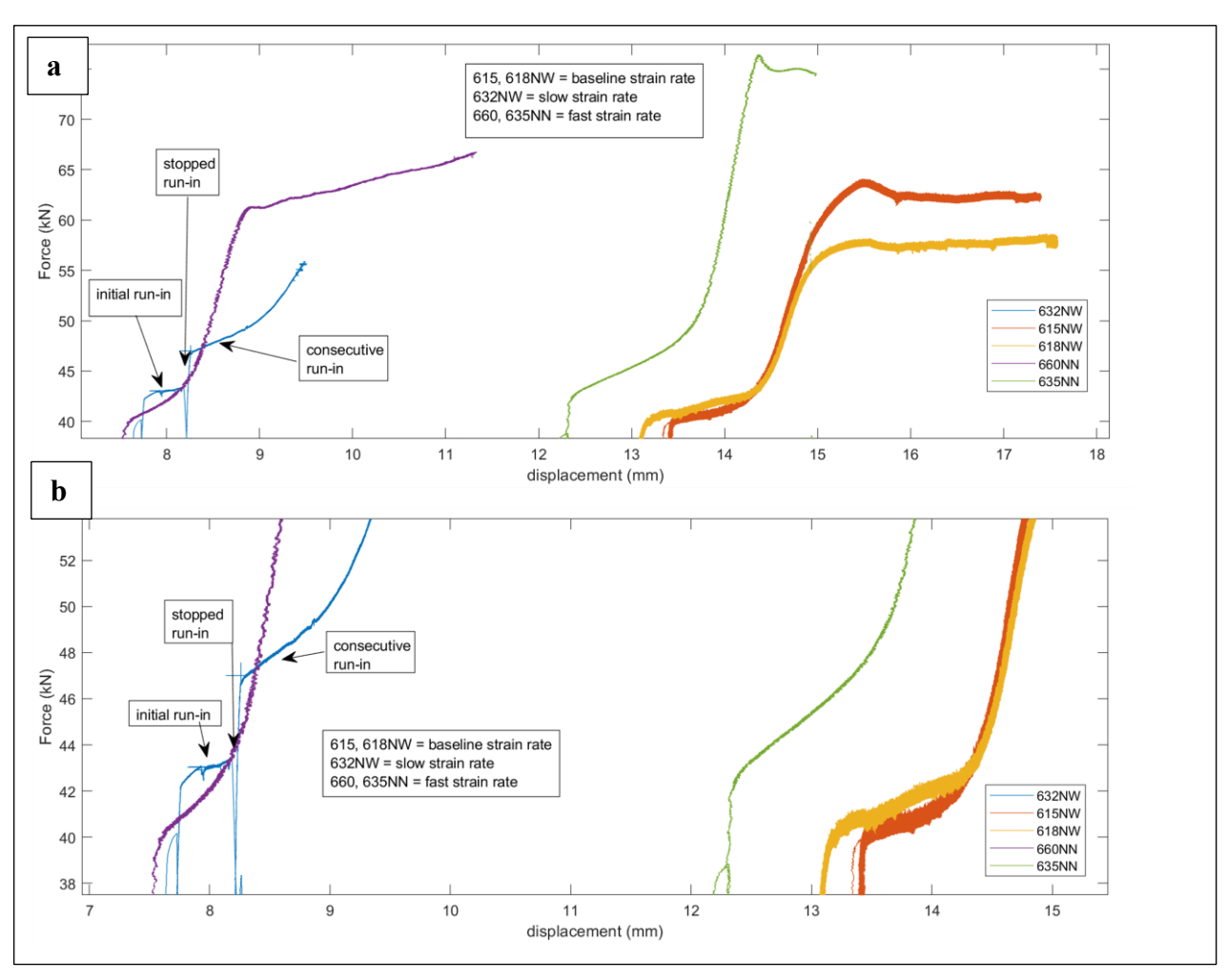


Figure S3: Comparison of the measured forces during experiments at different strain rates. The vertical piston displacement rates are defined as follows: for the baseline strain rate  $\approx 10^{-8}$ m/s, slow strain rate  $\approx 10^{-9}$ m/s and fast strain rate  $\approx 10^{-7}$ m/s. 1A is the overview and 1B is zoomed into the run-in curves of the experiments.

Three different vertical displacement rates were used in Fig. S3. The experiments 618NW and 615NW are performed with 10<sup>-8</sup>m/s, experiments 660NN and 635NN are one order of magnitude faster at 10<sup>-7</sup>m/s, and 632NN

one order of magnitude slower at  $10^{-9}$ m/s. Despite the different strain rates the run-in force of experiment 660NN is comparable to 615NW and 618NW. The run-in force of 635NN, however, is  $\approx$ 5kN higher than the same strain rate experiment 660NN, and the slower strain rate experiments 615NW and 618NW. The slow strain rate experiment 632NN shows a different trend: First, it is performed on another rig and secondly, there are two values for the run-in force. The reason for the two values (see Fig. S3b) is that there was a cooling problem during runin, and the experiment was stopped and restarted. Once experimental conditions were reached again, the slope was different from the initial run-in. Thus, we raise the question whether a calibration of different run-in values by hit-point stepping is even reliable within a single experiment?

Based on the observations on the larger dataset of M. Pec 2014, we still assume a base-force from the hit-point even for stepping experiments, because the slope of the run-in appears to be unreliable as a calibration tool altogether.

S4 Example error calculations for various shear zone heights and angles.

Table S2: Colours in the table are differentiating between different heights, hues of these colours guide through three different angles. D = vertical shortening of the cylinder,  $\Delta L$  = offset along the shear zone.

Shear zone height (៱m)	D vertical (mm)	Shear angle ( <b>Á</b> )	gL (mm)	Time (h)	Shear strain $\gamma$	Shear strain rate $\dot{\gamma}$
10	3.5	30	1.52	52	151	8.10E-04
10	3.5	35	1.64	52	164	8.78E-04
10	3.5	45	1.75	52	175	9.35E-04
50	3.5	30	1.52	52	30	1.62E-04
50	3.5	35	1.64	52	32	1.76E-04
50	3.5	45	1.75	52	35	1.87E-04
100	3.5	30	1.52	52	15	8.10E-05
100	3.5	35	1.64	52	16	8.78E-05
100	3.5	45	1.75	52	17	9.35E-05

## S5 Verification of flow law parameters

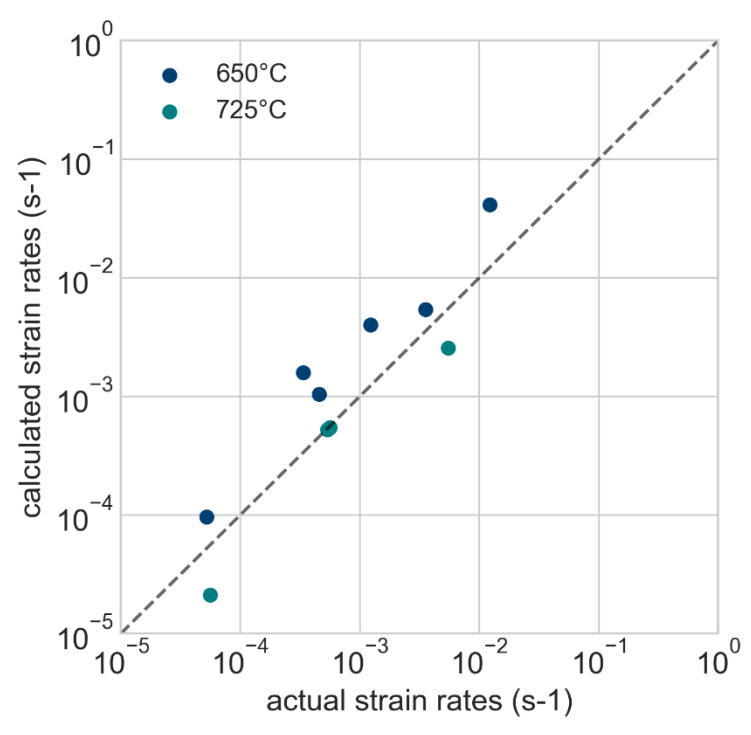


Figure S4: Actual and calculated strain rate values are plotted against each other. Calculated values are the values used for extrapolations in the main text: n=1.47, m=1.66, Q=167 kJ/mol, A=49.4 MPa<sup>-n</sup>  $\mu$ m<sup>m</sup> s<sup>-1</sup>.